Spectroscopic and Structural Characterization of Formazanyl Copper Complexes

Yoshiko KAWAMURA,* Jun YAMAUCHI, and Hiroaki OHYA-NISHIGUCHI†
Graduate School of Human and Environmental Studies, Kyoto University, Kyoto 606
† Institute for Life Support Technology, Yamagata Technopolis Foundation, 683 Kurumanomae, Numagi, Yamagata 990
(Received May 28, 1993)

1-(*o*-Substituted phenyl)-3,5-diphenyl-5-formazans form various kinds of complexes. The copper(II) complexes of 1,3,5-triphenyl-5-formazan and 1-(*p*-Cl and *o*-CH_3)-3,5-diphenyl-5-formazans (Group I) showed about 0.012 cm^{-1} of the parallel component of the copper(II) ESR splitting constant; those of the copper(II) complexes of 1-(*o*-Cl and *o*-Br)phenyl-3,5-diphenyl-5-formazans (Group II) were 0.018 cm^{-1}. The *f*-values in the near-infrared region of the former complexes were almost 10-times larger than those of the latter complexes. The difference was attributed to a tetrahedral distortion of about 65—70 degrees from the planar structure in Group I; the complexes of Group II, however, were almost planar. The complexes of 1-(*o*-OH and *o*-COOH)phenyl-3,5-diphenyl-5-formazans (Group III) showed exchange interactions between two copper(II) ions with exchange energies of −375 and +33.5 cm^{-1} for the former and the latter complexes of Group III, respectively. Referring to the exchange and dipolar interactions, the Cu–Cu distances and the Cu–O–Cu bridging angles are discussed.

The ligand configuration in copper(II) complexes has been studied with biological interest for a long time.[1—3] Many of them have helped in our understanding of the copper(II) environment at the active sites of copper-(II)-containing proteins. However, the results of electron spin resonance(ESR) and magnetic-susceptibility measurements have sometimes revealed different kinds of the copper(II) circumstance in the complexes.[4]

The authors have reported previously that the ESR behaviors of copper(II) complexes of formazan are greatly influenced by the *ortho*-substituent of the 1-phenyl ring of 5-formazan (Fig. 1).[5,6] The following is a summary of the previously reported results: (1) In accordance with the stoichiometries of the copper-(II) ion and formazan as well as the values of the ESR splitting constants of the copper(II) ion, the copper-(II) formazanato complexes were classified into three groups: In Group I, the stoichiometry of the copper(II) ion and formazan was 1 : 2 and the splitting constants of the copper(II) ion were small compared with those of the copper(II) complexes with the planar structure. In Group II, although the stoichiometry was also 1 : 2, the splitting constants were normal, similar to the values of complexes having a planar structure. In Group III, since the stoichiometry was 1 : 1, they would be of the dimer type. The splitting constants of a single copper-(II) ion were quite similar to those of Group II. (2) The structure around the copper(II) ion of all investigated copper(II) formazanato complexes was regarded to be basically planar, because their *g* values were similar to those with a planar structure.[7] (3) Groups I, II, and III nicely correspond to *Type 1*, *2*, and *3* copper(II)-containing proteins, respectively.[8—10]

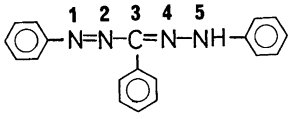

Fig. 1. 1,3,5-Triphenyl-5-formazan.

In order to probe the differences among the groups and to further study their characteristic properties, the magnetic study has been examined through the temperature dependence of magnetic-susceptibility measurements, and absorptions in the near-infrared region have been investigated. In addition, the ratio (R) of the parallel component of the g value ($g_{//}$) to also the parallel component of the copper(II) splitting constant ($A_{//}$) was examined. Referring to the R of other copper(II) complexes based on crystallographic data, the tetrahedral distortion angle of Group I was estimated to be 65—70 degrees, while the complexes of Group II and III were less distorted; both R and the oscillation strength (*f*-value) of the absorption band at around 825 nm showed a good correlation. It was verified that an increase in the d–d transition probability coincides with a distortion. On the other hand, the exchange interactions were observed in the complexes of Group III. Two copper(II) ions coupled antiferromagnetically in one complex and ferromagnetically in the other, as deduced from the exchange energy ($2J$). In addition, a different $2J$ was indicative of a difference in the Cu–O–Cu bridging angles caused by different *ortho* substituents. The experimentally obtained zero field splitting parameter (D), representing the dipolar interaction energy, enabled an estimation of the copper(II)–copper-(II) distance.[11] The diluted samples in the nickel(II) analogs served for an investigation of the configuration around the single copper(II) ion in the dinuclear complexes of Group III. Such a configuration difference of the copper(II) formazanato complexes will be discussed in relation to the *ortho* substituents.

Experimental

The samples used for physical measurements in the present study were bis[1,3,5-triphenyl-5-formazanato]copper-(II), **1**; bis[1-*p*-chlorophenyl-3,5-diphenyl-5-formazanato]-copper(II), **2**; bis[1-*o*-tolyl-3,5-diphenyl-5-formazanato]-copper(II), **3**; bis[1-*o*-chlorophenyl-3,5-diphenyl-5-for-

mazanato]copper(II), **4**; bis[1-*o*-bromophenyl-3,5-diphenyl-5-formazanato]copper(II), **5**; bis[1-*o*-oxyphenyl-3,5-diphenyl-5-formazanato]dicopper(II), **6**; and bis[1-*o*-carboxyphenyl-3,5-diphenyl-5-formazanato]dicopper(II), **7** (Fig. 2). Their preparation methods were the same as those for ESR measurements in a previous paper.[12] Nickel(II) analogs of **6** and **7** were prepared by using nickel(II) acetate following a similar method as that for the copper(II) complexes. Their elemental analyses were well fitted with the data of the calculated values within the experimental error. The stoichiometries of the copper(II) ion and formazan (experimentally obtained) were 1:2 in **1**, **2**, **3**, **4** and **5**, and 1:1 in **6** and **7**. Since the magnetism of the nickel(II) analogs was diamagnetic within the temperature range of the physical measurements, the copper(II) complexes diluted in the nickel(II) analog were synthesized in order to obtain information concerning the single copper(II) ion in the dimer environment. The ratio of copper(II) to nickel(II) ion was 1:50.

The magnetic-susceptibility measurements were carried out as functions of the temperature using a torsion balance (described elsewhere[13]); the data were corrected for the diamagnetism and temperature-independent paramagnetism (TIP). The molar magnetic-susceptibility (χ_M) was reported for **1**, **2**, and **7** previously.[5] The ESR spectra were recorded on a JEOLCO ME 3X spectrometer equipped with 100 kHz field modulation in the temperature range from room temperature to 4.2 K. The absorption spectra were recorded for a dichloromethane solution in the 340—2200 nm range using a Shimadzu Multi-purpose Spectophotometer (MPS50L).

Results and Discussion

Magnetic-Susceptibility Measurements. The temperature dependence of the magnetic susceptibility of **1**, **2**, and **3** was paramagnetic down to helium temperature and conformed to Curie–Weiss's law. An effective magnetic moment (μ_{eff}) of **3**, obtained from the gradient of the inverse molar susceptibility (χ_M^{-1}) vs. temperature (T) was 1.8 BM. μ_{eff} of **1** and **2** was 1.8 BM, as previously reported. These effective magnetic moments correspond to the value of the single spin of a copper(II) ion of $S=1/2$, indicating that the exchange interactions among the copper(II) ions are very weak. Complexes **4** and **5** in Group II were also paramagnetic over the entire range of the susceptibility measurements; their magnetic moments were 1.61 and 1.55 BM, respectively. Though their effective magnetic moments are slightly smaller than that of the free spin, the copper(II) ions do not interact. Groups I and II are, therefore, an isolated system of the copper(II) ion.

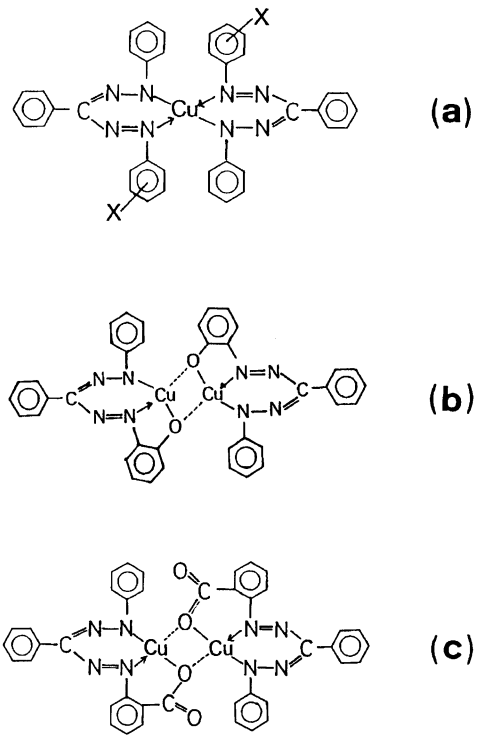

Fig. 2. Chemical structures. (a) **1**, **2**; X=*p*-Cl, **3**; X=*o*-CH_3, **4**; X=*o*-Cl, **5**; X=*o*-Br, (b) **6**, (c) **7**.

On the other hand, plots of χ_M of **6** versus the temperature showed a maximum at around 275 K, which decreased as the temperature decreased down to 77 K (Fig. 3). At 77 K the value of χ_M was only that of the temperature-independent paramagnetism. The solid curve in the figure represents the best fit of Bleaney–Bower's equation obtained, with $2J=-375$ cm^{-1} and $g_{av}=2.07$.[14]

$$\chi_M = \frac{Ng_{av}^2\beta^2}{kT \times (3+\exp(-2J/(kT)))} \quad (1)$$

Here, $2J$ is the exchange interaction energy between two copper(II) ions in a dinuclear complex and g_{av} is the averaged g value. The result of a magnetic-susceptibility measurement showed that since the copper(II) ions of **6** interact antiferromagnetically, the ground state is a singlet state. On the other hand, two copper(II) ions

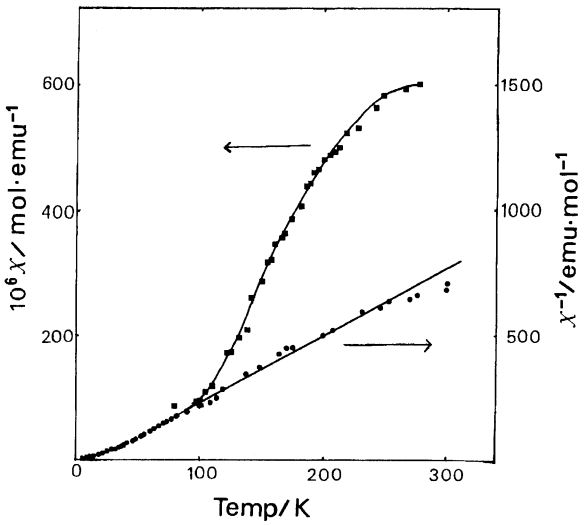

Fig. 3. Experimental and calculated temperature dependences of the molar magnetic susceptibility of **6** and the reciprocal molar magnetic susceptibility of **7**; $2J=-375$ cm^{-1}; $g=2.07$ for **6** and $2J=33.5$ cm^{-1}; $g=2.06$ for **7**. (■)**6**; (●)**7**.

in **7** interact ferromagnetically, as previosuly reported. The ground state of **7** is the triplet state since the positive $2J$ is indicative.[15] For a comparison, a $1/\chi_M$ vs. T plot of **7** is also shown in the same figure. The solid curve shows the best fit of the theoretical data with $2J=+33.5$ cm^{-1} and $g_{av}=2.06$. Thus, it was confirmed that **6** and **7** are dinuclear complexes of the copper(II) ions, as represented in Fig. 2. The dinuclear complex of the copper(II) ions is abbreviated as a dimer. The results of magnetic susceptibility measurements of seven complexes are summarized in Table 1.

ESR Results. Although the ESR results of the complexes of Groups I and II were previously reported, the results and discussion concerning the complexes of Group III were not sufficient. In the present paper, additional results and a more detailed discussion are represented concerning **6** and **7**.

ESR of 6: The ESR spectrum of a polycrystalline powder of **6** at room temperature (Fig. 4(a)) was a superposition of two kinds of absorptions; one is asterisked and the other is not. At liquid-nitrogen temperature, the former was scarcely recognizable, while the latter was emphasized due to its intensity. The spectrum at liquid-nitrogen temperatue is shown in Fig. 4(b), where the spectrum with 15-times intensity strength was added in order to emphasize the absorption at a magnetic field of 106 mT. The expanded spectrum of the central part is also represented in Fig. 4(c).

The asterisked resonance lines in Fig. 4(a) were assigned as being those due to the copper(II) dimer with the excited triplet state, which was derived from magnetic-susceptibility measurements. The zero-field splitting parameter of the triplet state was thus estimated; D^*, the zero-field splitting parameter found by a computer simulation, was 0.22 cm^{-1} for **6**, and D, obtained from the intervals between each pair of the absorptions (Fig. 4(a)), was 0.21 cm^{-1}.[16,17] On the other hand, a forbidden transition was observed at the magnetic field, H_{half}; the zero-field splitting parameter (D') was calculated following Eq. 2.[18] For complex **6**, H_{half} and g_{av} were 106 mT and 2.07, respectively. Here, the xy symmetry ($E=0$), was approximated under consideration of similar values of g_x and g_y, and ν was the microwave frequency. As a result of the calculation, D' was 0.209 cm^{-1}.

$$H_{half} = \frac{1}{g\beta}\left\{\left(\frac{h\nu}{2}\right)^2 + \frac{(D')^2 + E^2}{3}\right\}^{1/2} \quad (2)$$

Since D^*, D', and D were in good agreement, the zero-field splitting parameter of **6** was determined to be 0.21 cm^{-1}. At the same time, absorption at a magnetic field of 106 mT was confirmed to be the forbidden transition. The zero-field splitting parameters is listed in Table 2.

The spectrum of Fig. 4(c) is attributed to the paramagnetic part, due to the copper(II) monomer species. As the result of a computer simulation, g_z was 2.17 and, arbitrarily, $g_x=2.03$ and $g_y=2.01$. The parallel component of the copper(II) hyperfine splitting gave 0.018 cm^{-1}. These values are quite similar to those of the complexes of Group II. The configuration around the copper(II) ion in **6** would thus be similar to that of Group II. Besides, the perpendicular components of the copper(II) further split into 0.0017 cm^{-1} intervals, as is shown in Fig. 4(c). A computer simulation revealed that these were a superpositon of the perpendicular components of the copper(II) hyperfine splitting and the superhyperfine splitting due to the two ligand nitrogens.

ESR of 7: During ESR measurements of **7**, only one absorption at $g=2.06$ was observed, and no hyperfine splitting appeared both in a microcrystalline powder and a toluene solution at room temperature or liquid-nitrogen temperature.[19] They did not yield any structural information around the copper(II) ion. Even in the ESR in a microcrystalline powder at liquid-helium temperature, neither the fine structure nor the hyperfine structure was resolved in the broad absorption line. However, the resonance line ascribed to the forbidden transition due to the triplet state of the copper(II) dimer was observed at a magnetic field of 156 mT in a microcrystalline powder of **7** at 4.2 K (Fig. 5). Though the absorption line is located at a quite similar magnetic field, at which contaminated Fe^{3+} impurity absorption of $g=4.2$ is observed, it is clearly due to the half resonance, since it was observed under the conditions of the ESR amplitude and modulation at which Fe^{3+} ESR is never observed. The zero-field splitting parameter (D') was then calculated following Eq. 2 by the use of 156 mT of H_{half}, giving 0.020 cm^{-1}. Since

Table 1. Magnetic Data of Seven Complexes

Complexes	μ_{eff}/BM	Magnetism	Weiss's constant/K
1	1.8	para[a)]	−4*
2	1.8	para	−4*
3	1.8	para	−3
4	1.6	para	−2
5	1.6	para	−2
6		diamag[b)]	
7	1.8	ferromag[c)]	12*

*) Reportred in Ref. 5. a), b) and c) are the abbreviations of paramagnetic, diamagnetic, and ferromagnetic interactions.

Table 2. Exchange Energies and Zero-Field Splitting Parameters

Complexes	g_{av}	$2J$/cm^{-1}	D/cm^{-1}
6	2.07	−375	0.21
7	2.06	33.4	0.019
$Cu(CH_3COO)_2H_2O$[a)]	2.13	−284	0.35

a) Ref. 22.

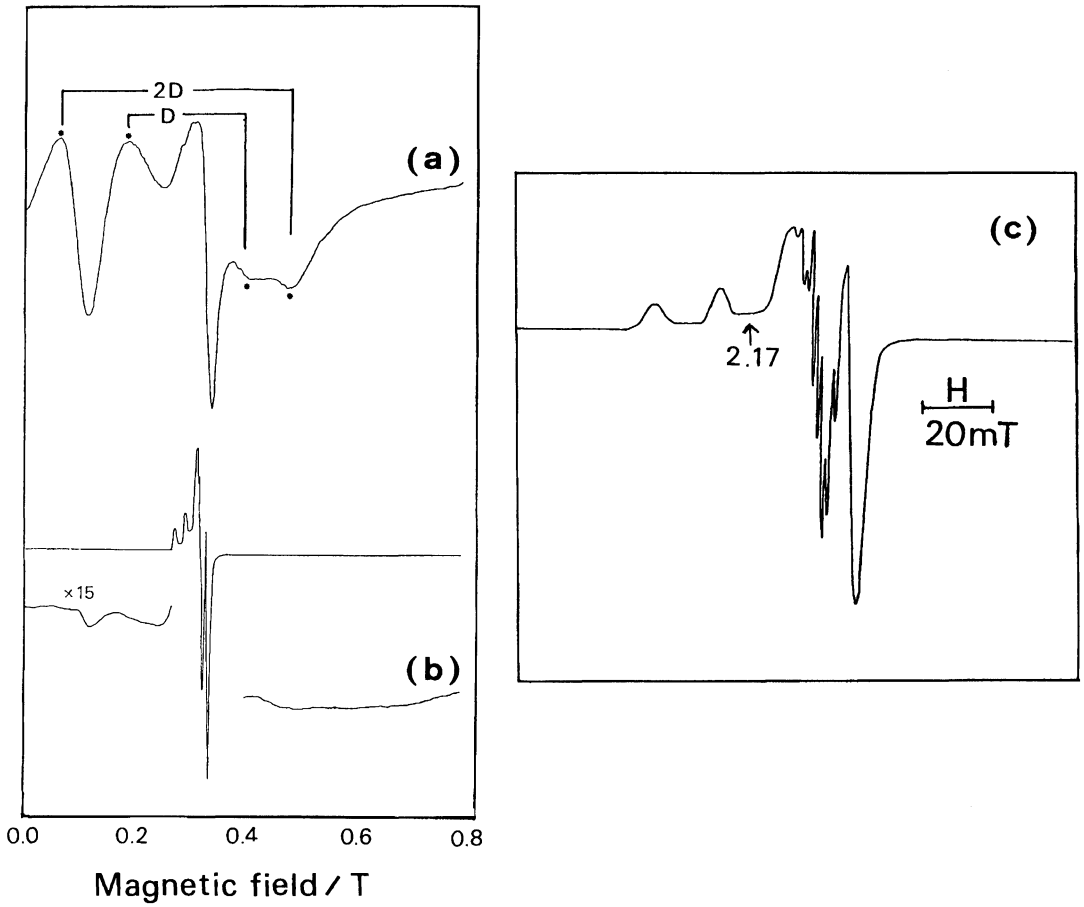

Fig. 4. ESR spectra of a microcrystalline state of **6** at (a) room temperature, and (b) liquid-nitrogen temperature. (c) is the expanded spectrum of (b) around $g=2$.

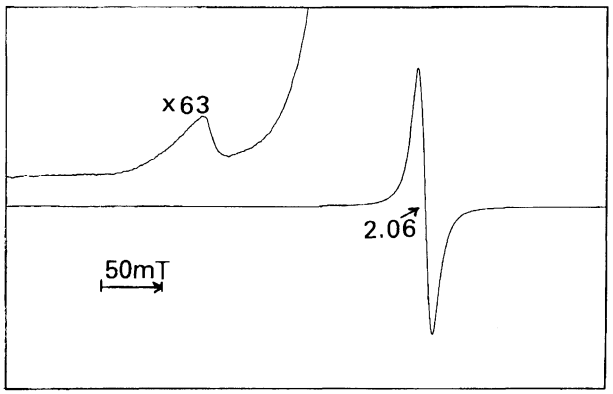

Fig. 5. ESR spectrum of a microcrystalline state of **7** at 4.2 K.

the temperature dependence of the magnetic-susceptibility measurements of **7** was well interpreted with the equilibrium between the ground triplet and the excited singlet states, the increase of the number in the ground triplet state at liquid-helium temperature would yield the ESR observation at H_{half}. Thus, the observation of the forbidden transition confirmed the ground triplet state, which was derived in the magnetic-susceptibility measurements.

ESR in a toluene solid solution at 4.2 K seemed to peek out the fine structure of the triplet state, as the result of a narrowing due to dilution. The D-value estimation from the intervals of each pair of the shoulders in Fig. 6 gave 0.019 cm^{-1}. Two values (D' of 0.020 cm^{-1} and D of 0.019 cm^{-1}) were well fitted within the experimental error. Thus, D of **7** is much smaller than that of **6**, giving a not very well-resolved fine structure. It can be conclusively said that only one resonance line in both the toluene solution and the microcrystalline powder at room temperature and liquid-nitrogen temperature would have been the consequence of an exchange interaction between two copper(II) ions and the small D value in the copper(II) dimer. The D of **7** are also given in Table 2.

ESR of Group III in the Nickel(II) Diluted System: Diluted systems of **6** and **7** in the nickel(II) analogs were prepared. It was confirmed that the nickel(II) ions had no spin in either complex. One of the nickel(II) ions in the nickel(II) dimer was substituted by the copper(II) ion, and ESR absorption dut to single copper(II) ion was observed. The ESR spectra of the diluted samples of **6** and **7** were similar to that of Fig. 4-(c); their ESR parameters were also similar to those of the complexes of Group II. The configuration around a

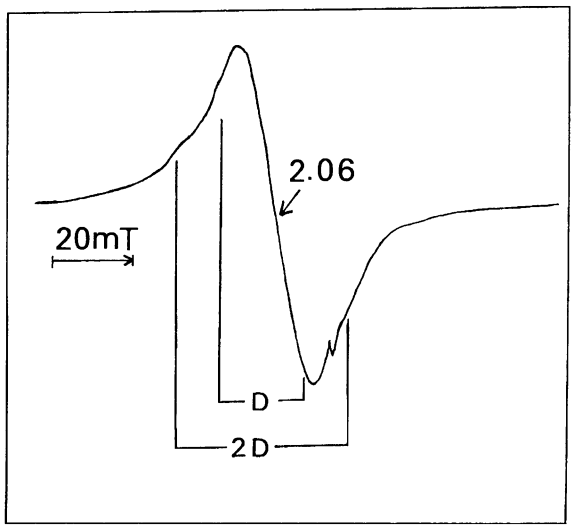

Fig. 6. ESR spectrum of a toluene solid solution of **7** at 4.2 K.

copper(II) ion in the dimer is also quite similar to those of the complexes of Group II.

Cu–Cu Distance and Bridging Angle. Referring to the D value, the Cu–Cu distance in the dimer was estimated. In the case that the exchange interaction is stronger and its energy is not negligible, the distance depends upon not only the dipolar interaction energy, but also the exchange interaction energy.[20] For such a case, one of the authors approximated the Cu–Cu distance (r) in the following relation:[21]

$$D = \alpha r^{-3}. \quad (3)$$

The coefficient α, which contains contributions from both D(dipole) and D(exchange), is deduced using D and r which are determined from ESR and X-ray experiments, respectively, following Eq. 3.[22] In the case of **6**, the D and J values are similar to that of Cu(II) acetate monohydrate (summarized in Table 2), although the bonding type around the Cu(II) ion is different. The α value was calculated for Cu(II) acetate monohydrate; then, using this α value and the experimentally obtained D, the Cu–Cu distance for **6** was estimated as to be 0.311 nm.

On the other hand, it is well known that two kinds of interactions, antiferromagnetic and ferromagnetic, are observed through superexchange interactions, depending on the bridging angle.[23,24] Hatfield et al. deduced the two relations concerning the J value based on the Cu–Cu distance and the Cu–O–Cu angle for hydroxo-bridged copper(II) dimers, based upon the structural and magnetical data.[25] Following their relations, the Cu–Cu distance and the Cu–O–Cu angle of **6** were 0.300 nm and 102 degrees. This distance is in good agreement with that determined from Eq. 3, 0.311 nm. The fact that the distances estimated by two methods were in good agreement with each other would mean that Hatfield's empirical relation also contains contributions from both J and D. The Hatfield relation can also be applicable to complex **7**. The Cu–Cu distance and the Cu–O–Cu angle of **7** were estimated to be 0.289 nm and 97 degrees, respectively.

It was reported that a bridging angle of about 97 degrees is the empirical boundary between antiferromagnetic and ferromagnetic interactions.[25—27] The Cu–O–Cu angle estimated in **7** is just on such a boundary, managing to yield a ferromagnetic interaction. Thus, depending upon the *ortho* substituent of the 1-phenyl ring of 1,3,5-triphenyl-5-formazan, the critical difference in the Cu–O–Cu angle has been produced and caused the antiferromagnetic interaction in **6** and the ferromagnetic interaction in **7**.

Optical Absorptions and Distortion. The ligand formazan has not only strong absorption at 585 nm, but the absorptions in the visible region of the complexes are also strong. Their absorption coefficients are 5000—6000 $mol^{-1}\,cm^{-1}$. They were therefore attributed to the charge-transfer bands from the ligand formazan to the copper(II) ion. On the other hand, since the absorptions in the NIR region of the complexes were broad and weak, they were ascribed to the d–d transition bands in the copper(II) ion. Representative absorption spectra are shown in Fig. 7. Two absorptions (**A** and **B**) were recognized in each complex; **A** is at about 820 nm and **B** is at around 1200 nm. **B** was not adequate for any further discussion, since they were too weak and broad. Thus, the absorption **A** served for a detailed consideration. Though the d–d transition probability is probably small, the tetrahedral distortion would increase the transition probability as the result of d-orbital mixing.[28] The absorption bands in NIR were very broad and weak, changing from sample to sample. The oscillation strength (f), defined as Eq. 4, was thus adopted for a comparison,[29]

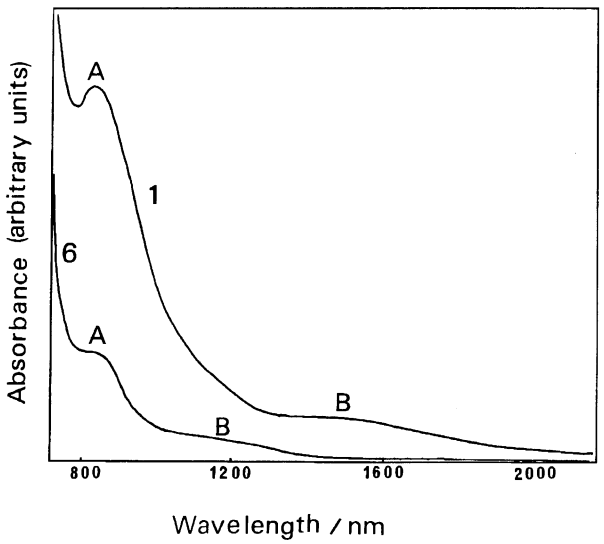

Fig. 7. Absorptions of **1** and **6** in the NIR region.

$$f = 4.32 \times 10^{-9} \times \int_{\nu_1}^{\nu_2} \epsilon(\nu)\mathrm{d}\nu. \quad (4)$$

The increase in the *f*-value indicates an increase in the d–d transition, which is caused by a greater tetrahedral distortion from a planar structure. The *f*-values of **A** of **1**, **2**, and **3** were 5.4×10^{-1}, 3.3×10^{-2}, and 3.1×10^{-2}, respectively. They were almost 10-times larger than those of the complexes of Groups II and III. This finding suggests that a greater distortion is produced in Group I than in Groups II and III.

The *R* also gives an estimation concerning the tetrahedral distortion.[30—34] Although the configuration is almost planar in the case that *R* is within the range of 115—135, the larger *R* corresponds to a greater tetrahedral distortion. The *R* values of Group I are more than 160, and those of Groups II and III are within 120—134 (Table 3). It is mentioned that Group I is not planar and Groups II and III are clearly planar. Gouteron correlated the tetrahedral angle (ω; Fig. 8) and *R*.[35] Referring to their correlation, the ω of Group I is estimated to be about 65—70 degrees, and that of Groups II and III is about 30—40. Group I is therefore rather tetrahedral and, on the contrary, Groups II and III are almost planar.

Now, a larger *R* corresponds a greater distortion, and an increase in *f*-value also indicates greater distortion. The *R* values of Groups I, II, and III were plotted versus the *f*-value (Fig. 9). They are in good correspondence. Thus, it is conclusively mentioned that the *f*-value, itself, enables an estimation of the degree of distortion.

Table 3. Spectroscopic Data of Absorption *A* and Ratio *R*

Complexes	Wavelength/nm	*f*-value	$R(=g_{//}/A_{//})$
1	837.5	5.4×10^{-2}	184
2	812.5	3.3×10^{-2}	175
3	825	3.1×10^{-2}	161
4	825	4.1×10^{-3}	125
5	825	2.3×10^{-3}	121
6	825	1.0×10^{-3}	120[a]
7	800	3.0×10^{-3}	134[a]

a) These *R* values were estimated for the nickel(II) diluted systems.

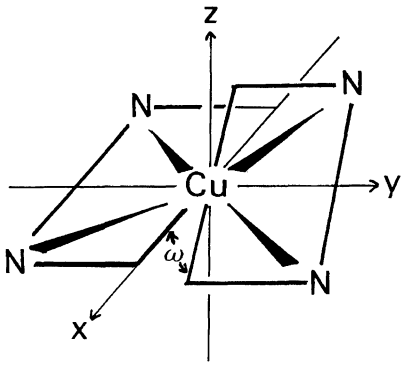

Fig. 8. Tetrahedral distortion angle from the planar structure.

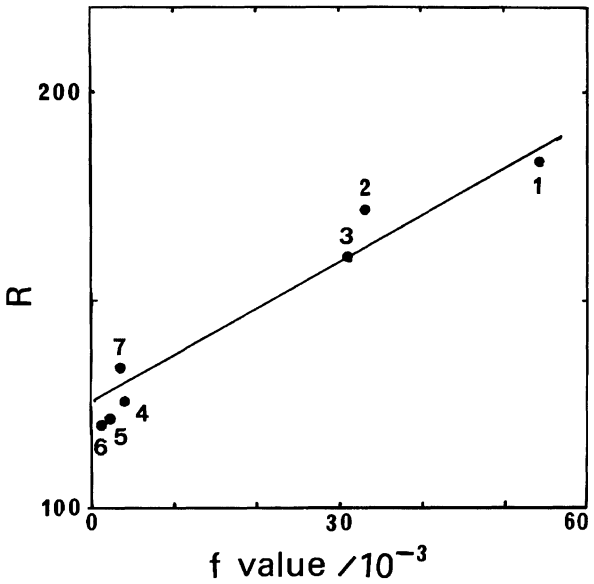

Fig. 9. Plots of *R* versus the *f*-values of the absorption *A* of the present complexes. The solid line was drawn by the least-squares method.

Finally, it would be interesting to note that an *ortho* substituent, such as chlorine or bromine in the 1-phenyl ring of 1,3,5-triphenylformazan, functions to maintain the planarity around the copper(II) ion in Group II. In Group III, furthermore, the bridging oxygen provided by the *ortho* substituents would work to maintain the planarity around the copper(II) ion. On the other hand, in Group I, in which 5-formazans do not have electronegative *ortho* substituents in 1-phenyl ring, nothing helped to maintain the planarity around the copper(II) ion. Thus, the 5-formazanato copper(II) complexes have a characteristic feature such that an *ortho* substituent in the 1-phenyl ring of 1,3,5-triphenyl-5-formazan enables a variety of configurations around the copper(II) ion. Such flexibility of the configuration around the copper(II) ion may cause some difficulty concerning their crystal growth of 5-formazanato copper(II) complexes.

Conclusion. The differences in three groups of 5-formazanato copper(II) complexes could be well interpreted in relation to the structural characterization of each Group, as follows. Two kinds of stoichiometry led to two kinds of interactions among the copper(II) ions: although in Groups I and II, the copper(II) ions do not interact with each other, in Group III two copper(II) ions do interact. Depending upon the bridging angle of Cu–O–Cu, antiferromagnetic and ferromagnetic interactions made their appearence in Group III. On the other hand, the difference in the ESR splitting constant between Group I and Groups II and III was deduced to the degree of the tetrahedral distortion from the planar structure.

References

1) U. Sakaguchi and A. W. Addision, *J. Chem. Soc., Dalton Trans.*, **1979**, 600.

2) D. E. Wilcox, J. R. Long, and E. I. Solomon, *J. Chem. Soc.*, **106**, 2186 (1984).

3) H. P. Berende and D. W. Stephan, *Inorg. Chem.*, **76**, 749 (1987).

4) For example: W. Zazurek, K. J. Berry, K. S. Murray, M. J. O'connor, M. R. Snow, and A. G. Wedd, *Inorg. Chem.*, **21**, 3071 (1982).

5) Y. Kawamura, H. O. Nishiguchi, J. Yamauchi, and Y. Deguchi, *Bull. Chem. Soc. Jpn.*, **57**, 7441 (1984).

6) Y. Kawamura, Y. Deguchi, J. Yamauchi, and H. O. Nishiguchi, *Bull. Chem. Soc. Jpn.*, **61**, 181 (1988).

7) A. R. Siedle and L. H. Pignolet, *Inorg. Chem.*, **19**, 2052 (1980).

8) A. R. Amundsen, J. Whelan, and B. Bosnich, *J. Am. Chem. Soc.*, **99**, 6730 (1977).

9) M. T. Youinou, J. A. Osborn, J. P. Collin, and O. Lagrange, *Inorg. Chem.*, **25**, 453 (1986).

10) R. Malkin and B. G. Malmstrom, *Adv. Enzymol.*, **33**, 177 (1970).

11) E. Colacio, J. P. Costes, J. P. Lourent, J. Ruiz, and M. Sundberg, *Inorg. Chem.*, **30**, 1475 (1991).

12) J. N. Ashley and B. M. Assour, *J. Chem. Phys.*, **48**, 365 (1964).

13) M. Mekata, *J. Phys. Soc. Jpn.*, **17**, 796 (1962).

14) B. Bleaney and K. D. Bowers, *Proc. R. Soc. London, Ser. A*, **214**, 451 (1952).

15) J. J. Mooiji, A. A. Klassen, and E. de Boer, *Mol. Phys.*, **32**, 879 (1976).

16) E. Wasserman, L. C. Snyder, and W. A. Yager, *J. Chem. Soc.*, **41**, 1763 (1964).

17) A. Ozarowski and D. Reinen, *Inorg. Chem.*, **25**, 1704 (1986).

18) See, for example: J. E. Wertz and J. R. Borton, "Electron Spin Resonance-Elementary Theory and Practical Applications," McGrow Hill, Inc., New York (1972).

19) A. Bencini, M. D. Vaira, A. C. Fabretti, D. Gatteschi, and C. Zanchini, *Inorg. Chem.*, **23**, 1620 (1984).

20) H. Abe and J. Shimada, *J. Phys. Soc. Jpn.*, **12**, 1255 (1957).

21) J. Yamauchi and S. Yano, *Makromol. Chem.*, **189**, 930 (1988).

22) J. N. van Nieberk and F. R. L. Schoening, *Acta Crystallogra.*, **6**, 227 (1953).

23) E. D. Estes, W. E. Hatfield, and D. J. Hodgson, *Inorg. Chem.*, **13**, 1954 (1974).

24) B. Chiari, J. H. Helms, O. Piovesana, T. Tarantellia, and P. F. Zanazzi, *Inorg. Chem.*, **25**, 870 (1986).

25) V. H. Crawford, H. W. Richardson, J. W. Wasson, D. J. Hodgson, and W. E. Hatfield, *Inorg. Chem.*, **15**, 2107 (1976).

26) A. T. Casy, B. F. Hoskins, and F. D. Whillans, *J. Chem. Soc., Chem. Commun.*, **1970**, 904; B. F. Hoskins and F. D. Whillans, *J. Chem. Soc., Dalton Trans.*, **1975**, 1267.

27) J. A. Batnes, W. E. Hatfield, and D. J. Hodgson, *J. Chem. Soc., Chem. Commun.*, **1970**, 1593; J. A. Barnes, D. J. Hodgson, and W. E. Hatfield, *Inorg. Chem.*, **11**, 144 (1972).

28) J. Ferguson, *J. Chem. Phys.*, **40**, 3406 (1964).

29) A. L. Sklar, *Rev. Mol. Phys.*, **14**, 232 (1942).

30) R. J. Wasson, H. W. Richardson, and W. E. Hatfield., *Z. Naturforsch, B*, **32**, 551 (1977).

31) H. Yokoi, *Bull. Chem. Soc. Jpn.*, **47**, 3037 (1974).

32) H. Yokoi and A.W. Addison, *Inorg. Chem.*, **16**, 1341 (1977).

33) Y. Murakami, Y. Tamada, and K. Sakata, *Inorg. Chem.*, **10**, 1734 (1971).

34) I. Bertimi, G. Canti, R. Grassi, and A. Scozzafam, *Inorg. Chem.*, **19**, 2198 (1980).

35) I. Gouteron, S. Jeanin, Y. Jeanin, J. Livage, and C. Sanchez, *Inorg. Chem.*, **23**, 3387 (1984).